Appendix A

Derivation of the Nernst equation

Consider the general reaction [1, 2]

$$\nu_A A + \nu_B B + \cdots + e^-(\text{metal}) \rightleftharpoons \nu_C C + \nu_D D + \cdots, \tag{A.1}$$

where ν_i are the stoichiometric coefficients of the individual components i. With the *electrochemical potential* $\tilde{\mu}_i$ of component i being related to its chemical potential μ_i by

$$\tilde{\mu}_i = \mu_i + z_i F\phi, \tag{A.2}$$

where $z_i F\phi$ is the electrical energy of species i (z_i is the charge carried by i, F is Faraday's constant, and ϕ is the potential of the particular phase (electrode or solution) in which i resides), the electrochemical potentials of the reactants and products in the equilibrium described by Eq. (A.1) can be expressed as

$$\nu_A\tilde{\mu}_A + \nu_B\tilde{\mu}_B + \cdots + \tilde{\mu}_{e^-} = \nu_C\tilde{\mu}_C + \nu_D\tilde{\mu}_D + \cdots. \tag{A.3}$$

The different $\tilde{\mu}_i$ can be substituted according to Eq. (A.2):

$$\begin{aligned}\nu_A(\mu_A + z_A F\phi_s) + \nu_B(\mu_B + z_B F\phi_s) + \cdots + (\mu_{e^-} - F\phi_m)\\ = \nu_C(\mu_C + z_C F\phi_s) + \nu_D(\mu_D + z_D F\phi_s) + \cdots.\end{aligned} \tag{A.4}$$

Conservation of electrical charge requires that

$$\nu_A z_A + \nu_B z_B + \cdots - 1 = \nu_C z_C + \nu_D z_D + \cdots. \tag{A.5}$$

A.S.J.L. Bachmeier, *Metalloenzymes as Inspirational Electrocatalysts for Artificial Photosynthesis*, Springer Theses,
DOI 10.1007/978-3-319-47069-6

Rearrangement of Eq. (A.4), substitution into Eq. (A.5), and solving for $F(\phi_m - \phi_s)$ leads to

$$F(\phi_m - \phi_s) = \nu_A\mu_A + \nu_B\mu_B + \cdots + \mu_{e^-} - \nu_C\mu_C - \nu_D\mu_D. \tag{A.6}$$

With

$$\mu_i = \mu_i^0 + RT\ \ln a_i. \tag{A.7}$$

follows

$$\begin{aligned} F(\phi_m - \phi_s) = {} & \nu_A(\mu_A^0 + RT\ \ln a_A) + \nu_B(\mu_B^0 + RT\ \ln a_B) + \cdots + \mu_{e^-} \\ & - \nu_C(\mu_C^0 + RT\ \ln a_C) - \nu_D(\mu_D^0 + RT\ \ln a_D). \end{aligned} \tag{A.8}$$

Substitution of the term

$$F\Delta\phi^0 = (\nu_A\mu_A^0 + \nu_B\mu_B^0 + \cdots) - (\nu_C\mu_C^0 + \nu_D\mu_D^0 + \cdots) + \mu_{e^-}, \tag{A.9}$$

which is constant at a fixed temperature and pressure, into Eq. (A.8), and rearrangement lead to a general statement of the Nernst equation:

$$\phi_m - \phi_s = \Delta\phi^0 + \frac{RT}{F}\ln\left\{\frac{a_A^{\nu_A}a_B^{\nu_B}\cdots}{a_C^{\nu_C}a_D^{\nu_D}\cdots}\right\}. \tag{A.10}$$

For 'ideally' behaving solutions activities can be approximated to concentrations. With $E = \phi_m - \phi_s$ and $E^0 = \Delta\phi^0$, and by introducing z for the number of electrons transferred in the process (as a means of generalisation to account for processes with $z > 1$), Eq. (A.9) can be rewritten as

$$E = E^0 + \frac{RT}{zF}\ln\frac{[\mathrm{Ox}]}{[\mathrm{Red}]}, \tag{A.11}$$

which, when at equilibrium ($E = E_{eq}$), equates Eq. (2.7) in Sect. 2.2.4.

With the change in free energy ΔG being defined as the sum of the products of the stoichiometric coefficients ν_i and the chemical potentials μ_i of the individual components i

$$\Delta G = \sum \nu_i\mu_i, \tag{A.12}$$

the relationship between the Nernst equation and ΔG becomes apparent:

$$\Delta G = \sum \nu_i\mu_i^0 + RT\sum \nu_i \ln a_i \tag{A.13}$$

or, rearranged:

$$\Delta G = \Delta G^0 + RT \ln \prod_i [a_i]^{\nu_i}. \tag{A.14}$$

Hence,

$$\Delta G = -zFE. \tag{A.15}$$

Appendix B

Derivation of the Mott-Schottky Equation

Consider an n-type semiconductor under depletion [3]. The density of electrons and holes at the surface, n_s and p_s, respectively, is related to their constant bulk values by

$$n(x) = n_b e^{\frac{e_0 \Delta\phi}{k_B T}} \quad \text{and} \quad p(x) = p_b e^{-\frac{e_0 \Delta\phi}{k_B T}}, \tag{B.1}$$

where $\Delta\phi = \phi_x - \phi_b$ represents the surface-bulk potential difference, i.e. the band-bending, and n_b and p_b are the electron and hole concentrations in the bulk of the semiconductor. The potential, the charge density (ρ), and the number of carriers (n and p) all depend on the distance (x) away from the interface into the semiconductor bulk. The charge density in an n-type semiconductor can be expressed as [4]

$$\rho(x) = e_0(-n(x) + p(x) - N_A + N_D) \tag{B.2}$$

and $n \gg p$, $N_D \gg N_A$. Further, the density of electrons in the bulk principally equals the donor density, i.e. $n_b \approx N_D$. Using these simplifications, Eq. (B.2) can be rewritten as follows:

$$\rho(x) = e_0 N_D \left(1 - e^{\frac{e_0 \Delta\phi}{k_B T}}\right). \tag{B.3}$$

The charge density is related to the potential by the Poisson equation [5]:

$$\frac{d^2\phi(x)}{dx^2} = \frac{-\rho(x)}{\varepsilon_r \varepsilon_0}. \tag{B.4}$$

A.S.J.L. Bachmeier, *Metalloenzymes as Inspirational Electrocatalysts for Artificial Photosynthesis*, Springer Theses,
DOI 10.1007/978-3-319-47069-6

Using the substitution

$$v = -\Delta\phi = -(\phi_x - \phi_b) \tag{B.5}$$

Equation (B.4) can be expressed as

$$-\frac{d^2v}{dx^2} = -\frac{\rho(x)}{\varepsilon_r\varepsilon_0} \tag{B.6}$$

and substituted in Eq. (B.3):

$$\frac{d^2v}{dx^2} = \frac{e_0 N_D}{\varepsilon_r\varepsilon_0}\left(1 - e^{\frac{-e_0 v}{k_B T}}\right). \tag{B.7}$$

With the property of derivatives [5]

$$\frac{d^2v}{dx^2} = \frac{1}{2}\frac{d}{dv}\left(\frac{dv}{dx}\right)^2 \tag{B.8}$$

Equation (B.7) transforms into

$$d\left(\frac{dv}{dx}\right)^2 = \frac{2e_0 N_D}{\varepsilon_r\varepsilon_0}\left(1 - e^{\frac{-e_0 v}{k_B T}}\right)dv. \tag{B.9}$$

Integration gives

$$\left(\frac{dv}{dx}\right)^2 = \frac{2e_0 N_D}{\varepsilon_r\varepsilon_0}\left(v + \frac{k_B T}{e_0}e^{\frac{-e_0 v}{k_B T}}\right) + \text{const.} \tag{B.10}$$

Taking into account that in the bulk of the semiconductor ($x \to \infty$) $\phi_x = \phi_b$, i.e. there is no potential difference between two points ($v = 0$) and $\frac{dv}{dx} = 0$,

$$\left(\frac{dv}{dx}\right)^2 = \frac{2e_0 N_D}{\varepsilon_r\varepsilon_0}\left(v - \frac{k_B T}{e_0}\left(1 - e^{\frac{-e_0 v}{k_B T}}\right)\right). \tag{B.11}$$

At the surface with $x = 0$; $v = v_s$, the following approximation can be used for the depletion layer of the semiconductor:

$$v_s \gg \frac{k_B T}{e_0}. \tag{B.12}$$

Then, Eq. (B.11) simplifies to

$$\left(\frac{\mathrm{d}v}{\mathrm{d}x}\right)_{x=0} = \left(\frac{2e_0N_\mathrm{D}}{\varepsilon_\mathrm{r}\varepsilon_0}(v_\mathrm{s} - \frac{k_\mathrm{B}T}{e_0})\right)^{1/2}. \tag{B.13}$$

Using Gauss' law to express the total charge Q [4] as

$$Q = \varepsilon_r\varepsilon_0\left(\frac{\mathrm{d}v}{\mathrm{d}x}\right), \tag{B.14}$$

and combining Eqs. (B.13) and (B.14), Eq. (B.15) is obtained:

$$Q = \left(2\varepsilon_\mathrm{r}\varepsilon_0 e_0 N_\mathrm{D}(v_\mathrm{s} - \frac{k_\mathrm{B}T}{e_0})\right)^{1/2}. \tag{B.15}$$

The interfacial capacitance of the space-charge layer C_sc is given as

$$C_\mathrm{sc} = \frac{\mathrm{d}Q}{\mathrm{d}v_\mathrm{s}}. \tag{B.16}$$

Substitution of Eq. (B.15) into Eq. (B.16) and differentiation yields

$$C_\mathrm{sc} = \frac{\varepsilon_\mathrm{r}\varepsilon_0 e_0 N_\mathrm{D}}{\sqrt{2}\sqrt{\varepsilon_\mathrm{r}\varepsilon_0 e_0 N_\mathrm{D}\left(v_\mathrm{s} - \frac{k_\mathrm{B}T}{e_0}\right)}} = \left(\frac{2}{\varepsilon_\mathrm{r}\varepsilon_0 e_0 N_\mathrm{D}}(v_\mathrm{s} - \frac{k_\mathrm{B}T}{e_0})\right)^{-1/2}. \tag{B.17}$$

With $v_\mathrm{s} = 0$ at $E = E_\mathrm{fb}$

$$v_\mathrm{s} = E - E_\mathrm{fb}, \tag{B.18}$$

and Eq. (B.17) transforms into the Mott-Schottky equation Eq. (2.40) [3]:

$$C_\mathrm{sc}^{-2} = \frac{2}{\varepsilon_\mathrm{r}\varepsilon_0 e_0 N_\mathrm{D}}\left(E - E_\mathrm{fb} - \frac{k_\mathrm{B}T}{e_0}\right). \tag{B.19}$$

Appendix C

The Effect of H_2 Consumption by Ca*HydA at High Potential*

The effect of H_2 consumption by *Ca*HydA at oxidising potentials was determined by chronoamperometry, since in inhibition studies using acetaldehyde (described in Sect. 3.2.3) the gas flow had to be interrupted simultaneously to aldehyde injection, because of the high volatility of MeCHO (bp 20 °C). The figure below depicts three control experiments carried out analogously to the inhibition studies described in Sect. 3.2.3, apart from buffer solution being injected into the electrochemical cell at $t = 0$ instead of acetaldehyde (H_2 flow was turned off simultaneously to buffer injection; the electrode was poised at 0.0 V vs. SHE; $\omega = 3000$ rpm; pH 6.0 phosphate buffer; dark). In all three cases, less than 5% activity is lost during 5 min, the typical time-course of an actual inhibition experiment.

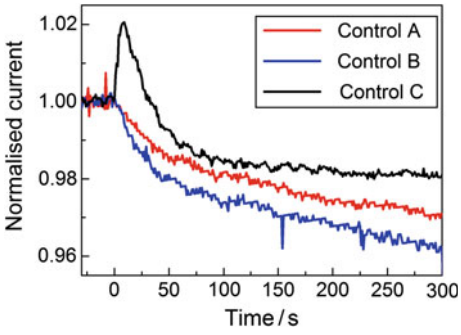

A.S.J.L. Bachmeier, *Metalloenzymes as Inspirational Electrocatalysts for Artificial Photosynthesis*, Springer Theses,
DOI 10.1007/978-3-319-47069-6

Appendix D

Continuous-Wave EPR Spectrum of Formaldehyde-Inhibited CrHydA1

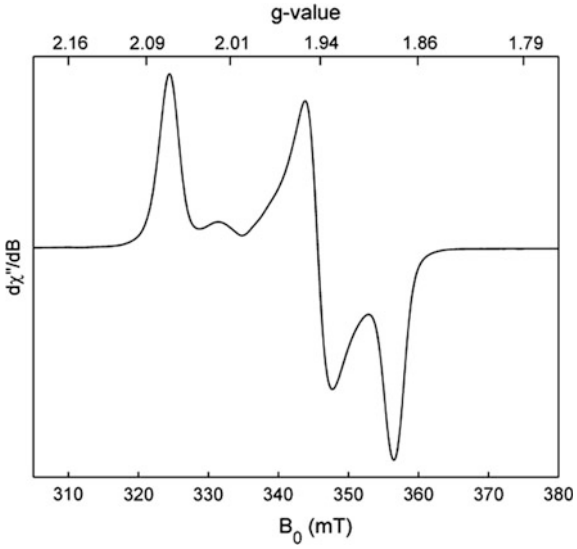

X-band EPR spectrum of formaldehyde-inhibited *Cr*HydA1 collected at 11 K, 9.3902 GHz, with a total spin concentration of 830 μM. Non-saturating conditions were employed, i.e. microwave power of 1 mW, modulation amplitude of 1 Gauss, and digital smoothing of 10 points of 1 point per Gauss in a sweep of 1500 G in 10 s. The minor signal at 330 mT (g = 2.025) most likely corresponds to a decay product following HCHO inhibition of *Cr*HydA1.

A.S.J.L. Bachmeier, *Metalloenzymes as Inspirational Electrocatalysts for Artificial Photosynthesis*, Springer Theses,
DOI 10.1007/978-3-319-47069-6

Appendix E

X-Band ENDOR Natural Abundance Carbon Control

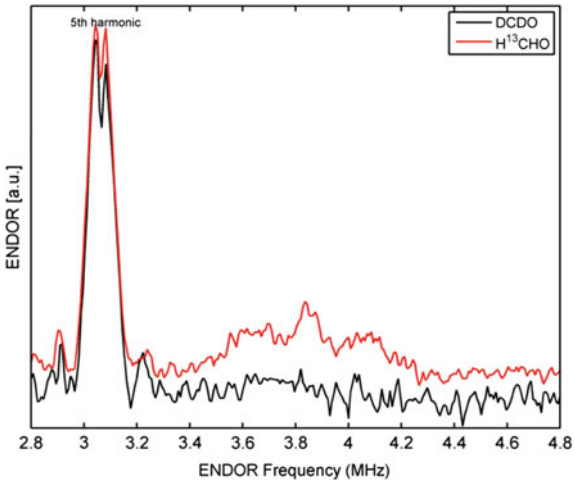

X-band ENDOR spectrum of a ^{2}H control, DCDO, with natural abundance carbon (i.e. approximately 99% ^{12}C), compared to formaldehyde isotopically labelled with ^{13}C. The two spectra are scaled to the 5th harmonic of the ^{1}H-ENDOR signal (as indicated in the figure). Data was collected at g = 1.944, under the same conditions as in Fig. 3.18. Reprinted with permission from [6]. Copyright 2016 American Chemical Society

A.S.J.L. Bachmeier, *Metalloenzymes as Inspirational Electrocatalysts for Artificial Photosynthesis*, Springer Theses,
DOI 10.1007/978-3-319-47069-6

Appendix F

Mott-Schottky Experiment on CODH–CdS

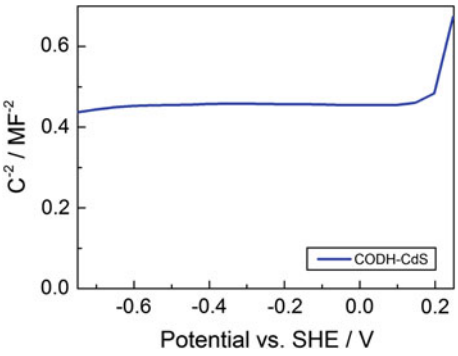

Mott-Schottky plot ($1/C^2$ vs. *E*) recorded at 20 °C, 1 kHz for CODH–CdS under 100% N_2 in a 0.2 M MES (pH 6.0) cell buffer solution.

A.S.J.L. Bachmeier, *Metalloenzymes as Inspirational Electrocatalysts for Artificial Photosynthesis*, Springer Theses,
DOI 10.1007/978-3-319-47069-6

Appendix G

Photoelectrocatalytic Fumarate Reduction Under Inverse Connections

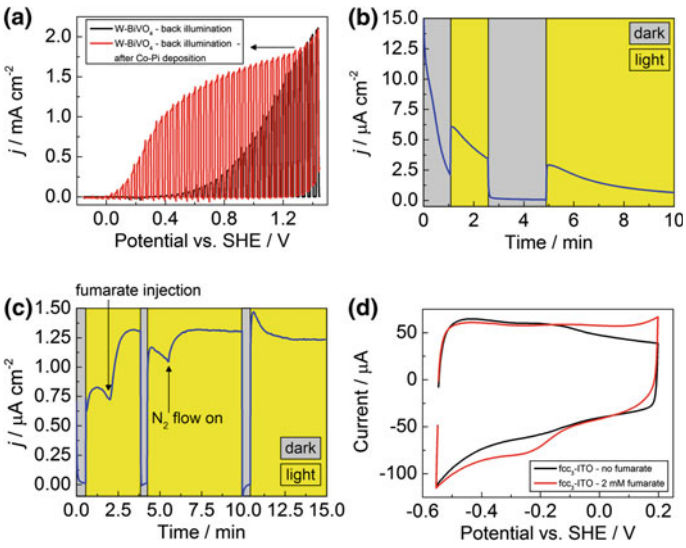

Photoelectrocatalysis experiment carried out with reversed connections, i.e. Co–Pi-W–$BiVO_4$ as the working electrode and fcc_3–ITO as counter. (a) Linear sweep voltammograms recorded before and after Co–Pi deposition on W–$BiVO_4$; 10 mV s^{-1}, chopped illumination (0.5 Hz, back illumination), 25 °C, 0.1 M KPi buffer (pH 7.0). (b) Current vs. time trace of the Co–Pi-W–$BiVO_4$ WE connected to the bare *meso*-ITO electrode (CE) in a two-compartment photoelectrochemical cell at zero external bias. Conditions: no gas flow, 25 °C, 0.1 M KPi buffer (pH 7.0). (c) Chronoamperometry experiment depicting photocurrent densities corresponding to visible-light-driven fumarate reduction; 25 °C, 0.1 M KPi buffer (pH 7.0). The

A.S.J.L. Bachmeier, *Metalloenzymes as Inspirational Electrocatalysts for Artificial Photosynthesis*, Springer Theses,
DOI 10.1007/978-3-319-47069-6

reduction compartment was sparged with N_2 to allow efficient substrate transport to the electrode, gas flow was turned off during injection of fumarate (final concentration 2 mM) into the reduction compartment at $t = 2.0$ min. (d) Cyclic voltammogram of fcc_3–ITO recorded after chronoamperometry experiments depicted in (c); 30 mV s^{-1}, 25 °C, 0.1 M KPi buffer (pH 7.0), N_2 flow. The red trace, recorded after introducing fumarate (final concentration 2 mM) into the solution, shows that the enzyme is still catalytically active towards fumarate reduction.

References

1. Compton RG, Banks CE (2011) Understanding Voltammetry, 2nd edn. Imperial College Press, London
2. Compton RG, Sanders GHW (1996) Electrode Potentials. Oxford University Press, Oxford
3. Gelderman K, Lee L, Donne SW (2007) J Chem Educ 84:685
4. Bockris JOM, Khan SUM (1993) Surface Electrochemistry: A Molecular Level Approach. Plenum Press, New York
5. Brett CMA, Oliveira Brett AM (1993) Electrochemistry: Principles, Methods, and Applications. Oxford University Press, Oxford
6. Bachmeier A, Esselborn J, Hexter SV, Krämer T, Klein K, Happe T, McGrady JE, Myers WK, Armstrong FA (2015) J Am Chem Soc 137:5381